Study of Heat and Particle Flux in the Case of Gas Injection in the D-Module of GAMMA 10/PDX*)

Md. Shahinul ISLAM, Yousuke NAKASHIMA, Hiroto MATSUURA[1)], Kazuya ICHIMURA, Md. Maidul ISLAM, Keita SHIMIZU, Kazuma FUKUI, Masato OHUCHI, Kunpei NOJIRI, Akihiro TERAKADO, Naomichi EZUMI, Mizuki SAKAMOTO and Tsuyoshi IMAI

Plasma Research Center, University of Tsukuba, Tsukuba, Ibaraki 305-8577, Japan

[1)]*Radiation Research Center, Osaka Prefecture University, Osaka 599-8531, Japan*

(Received 30 November 2015 / Accepted 3 March 2016)

This research investigated the radiation cooling mechanism and formation of detached plasma in the case of gas injection in the D-module of GAMMA 10/PDX. In GAMMA 10/PDX, divertor simulation experiments have been started by using a divertor simulation experimental module (D-module). A V-shaped target made of tungsten has been installed in this module. In order to understand the effect of impurity injection into divertor simulation experimental module, we injected H_2 and Ar gases to the D-module and measured the heat flux and ion flux. According to the increase of gas injection, reduction of ion and heat fluxes have been observed. In the Ar injection experiments, H_2 gas has been injected simultaneously to examine the effect of molecular process on detached plasma formation. In this case, both the heat flux and ion flux are drastically reduced. These results indicate radiation cooling and formation of detached plasma due to gas injection. Simultaneous injection of noble gas and hydrogen gas showed the most effective results on detached plasma generation.

Keywords: GAMMA 10/PDX, D-module, Detached plasma, Heat flux, Ion saturation current ($I_{\text{i-sat}}$), Electron temperature (T_e), Electron density (n_e)

DOI: 10.1585/pfr.11.2402042

1. Introduction

In toroidal fusion devices, reduction of heat load on to the target plate is one of the most important issues. The divertor is exposed to high heat load. In ITER discharges, the heat load to the divertor plate is estimated to be 5 - 10 MW/m^2 in steady state [1, 2]. For concentrated heat flux in divertor region, erosion and sputtering are produced on the divertor plate. Therefore, it is necessary to reduce heat load on to the target plate. Gas injection into a divertor plasma is one possible idea to reduce the heat load on divertor plates, since impurity gas causes radiative power loss and decreases electron temperature, expected to result in plasma detachment. GAMMA 10/PDX is the world's largest linear device which is 27 m long. It utilizes many plasma heating devices with the same scale of the present day fusion devices, such as Electron Cyclotron Heating (ECH), Ion Cyclotron Range of Frequency (ICRF), and Neutral Beam Injection (NBI) system [3, 4]. In GAMMA 10/ PDX, high heat and particle fluxes can be generated by applying ECH and additional ICRF waves (RF3) [5, 6]. The divertor simulation experimental module (D-module), in which a V-shaped target is mounted, was installed in the west end-cell of GAMMA 10/PDX [5–8]. It has been aimed to investigate the physics of radiation cooling and plasma detachment by impurity injection. In the D-module of GAMMA 10/PDX, it is necessary to investigate heat and particle flux by injecting impurity gas in order to realize detached condition. In this study, the plasma cooling mechanism towards the detached plasma has been investigated by injecting two types of gas (Ar, H_2). The purpose of this research is to investigate plasma behavior from the calorimeters and Langmuir probe's data in the case of gas injection for making into plasma detachment.

2. Experimental Setup

GAMMA 10/PDX is a tandem mirror device. Figure 1 (a) shows the schematic view of the GAMMA 10/PDX device and the experimental setup for the divertor simulation experiments. GAMMA 10/PDX consists of central-cell, anchor-cells, plug/barrier-cells and end-cells [9]. In GAMMA 10/PDX, divertor simulation experiments have been started by using a D-module. The D-module consists of a rectangular chamber (cross-section 50×50 cm and 100 cm in length) made of stainless steel. The D-module can be moved up and down by using an elevation system and placed on axis close to the end-mirror exit in the divertor simulation experiment. In this experimental module, as shown in Fig. 1 (b), two target plates (350×300 mm) are mounted in V-shaped with their variable open-angle from 15 to 80 degree. The D-module is

author's e-mail: shahinul@prc.tsukuba.ac.jp

*) This article is based on the presentation at the 25th International Toki Conference (ITC25).

equipped with three gas injection systems (H_2 gas for density build-up, noble gases (Ne, Ar, N_2, Xe) for radiation cooling and He gas for spectroscopy) in order to make realization of plasma detachment in the D-module.

Figure 1 (b) shows the schematic view of the V-shaped tungsten target and layout of diagnostic tools. A set of Langmuir probes and calorimeters has been installed at the upper and lower plates, respectively, of the V-shaped target for simultaneous measurement of particle and heat flux. A pair of calorimeter and Langmuir probe has also been installed behind a small gap of the V-shaped corner (Z = 1091 cm). 13 Calorimeters are installed to Y and Z direction on the target plate. The spatial distribution of heat flux along target plate is measured by the calorimeter under the conditions of target angle (α) of 30°, 45° and 60° [8]. In this experiment, we measured heat flux under the target angle of 45°. Fig. 1 (c) shows the schematic view of gas injection system in the D-module.

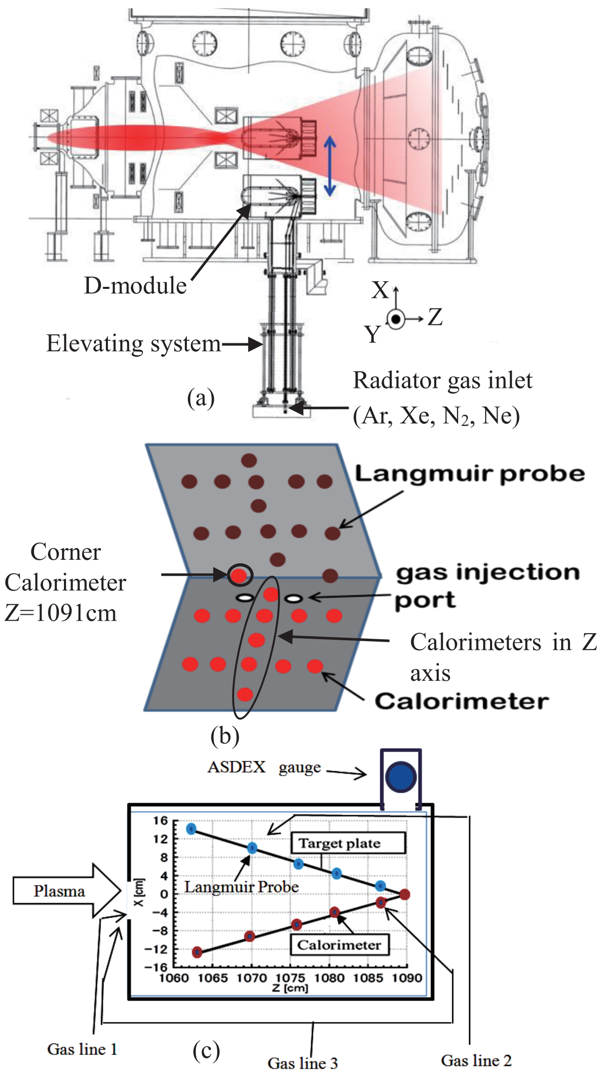

Fig. 1 Schematic view of (a) GAMMA10 West End-mirror cell. (b) V-shaped tungsten target and layout of diagnostic tools (c) gas injection system.

In this experiment, H_2 and Ar gases were injected by using gas line 1 and gas line 2, respectively. At present, the ASDEX gauge measurement is under calibration.

3. Experimental Results and Discussion

To investigate radiation cooling and formation of detached plasma in the D-module, hydrogen and argon gases were injected during plasma exposure. Due to the poor conductance of the gas injection system, the gases were injected sub seconds earlier than plasma ignition. The timing data of gas injection is listed in Table 1. The gas throughput into the D-module is controlled by changing the plenum pressure of gas reservoir.

The time behavior of the electron line-density and the diamagnetism measured in the central-cell is shown in Fig. 2. In the central-cell, main plasma is produced and heated by ICRF waves (RF1-2) together with gas puffing. A remarkable change in the electron line-density and the diamagnetism is observed during RF3 injection (t = 170 - 240 ms). RF3 is used for additional heating in the anchor-cell in order to build up particle flux at the end-cell [5, 6]. In the anchor-cell, ions are heated in the perpendicular to the magnetic field line and become trapped particles in the anchor mirror by RF3. Therefore, electron line-density increases in the anchor-cell. In this experiment, the increase of the line-density and decrease of the diamagnetism are observed might be due to the reduction of heating efficiency of RF2 in the central-cell [10–12].

The main plasmas consist of high density region and low density region plasmas. The heat flux includes both regions. The heat flux measured by calorimeter which is attached on the V-shaped target is evaluated from the temperature difference (ΔT) of the metal solid between before and after plasma discharge [8]. In this measurement, measuring error and reflection of flux by the surface is ignored.

Table 1 Gas timing.

Gas	Delay [s]	Pulse Width [s]
Ar	-0.45	0.3
H_2	-0.3	0.55

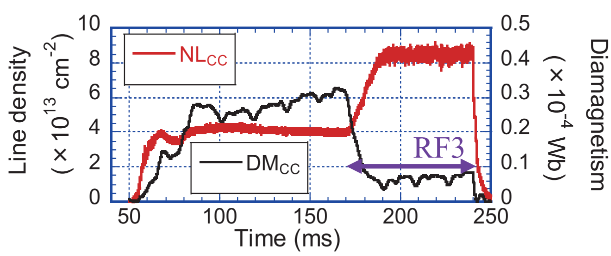

Fig. 2 Temporal behaviors of the electron line density, NL_{CC}, and the diamagnetism, DM_{CC}, measured in the central-cell. RF3 was applied from 170ms to 240 ms.

Time averaging values (100 - 150 ms: W/O RF3 and 190 - 240 ms: With RF3) of n_e, $I_{i\text{-sat}}$ and T_e have been used in this study because in these each region, plasma is almost stable.

3.1 H_2 gas injection

The distribution of heat flux on Z axis is plotted in Fig. 3. According to the increase of gas throughput, the heat flux is reduced. The heat flux decreases at all points during H_2 gas injection except for the plenum pressure of 200 mbar. Figure 4 shows the dependence of plasma parameters on the H_2 plenum pressure. According to the increase of H_2 gas injection, electron density and electron temperature near the corner of target decreases. At lower plenum pressure (≤ 400 mbar), it is observed that electron density increases almost linearly but at higher plenum pressure (> 400 mbar), electron density decreases.

The distributions of heat and ion fluxes at the corner of the target (Z = 1091 cm) as a function of plenum pressure are shown in Fig. 4 (b). As shown in Fig. 4 (b), it is observed that the heat flux decreases with the increasing plenum pressure. In this case, the heat flux at the corner of the target was reduced by about 10 times (0.034 MW/m^2 to 0.0034 MW/m^2). On the other hand, ion flux at the corner of the target was reduced by about 5 times (during RF3 injection). Ion flux shows a roll over phenomenon.

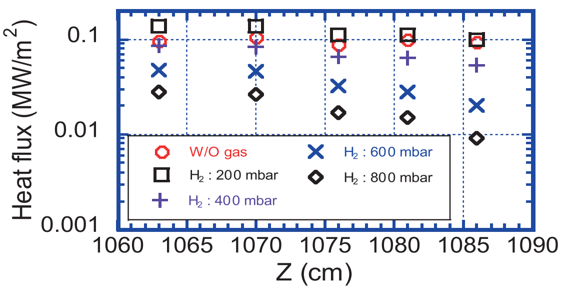

Fig. 3 Heat flux distribution on Z axis.

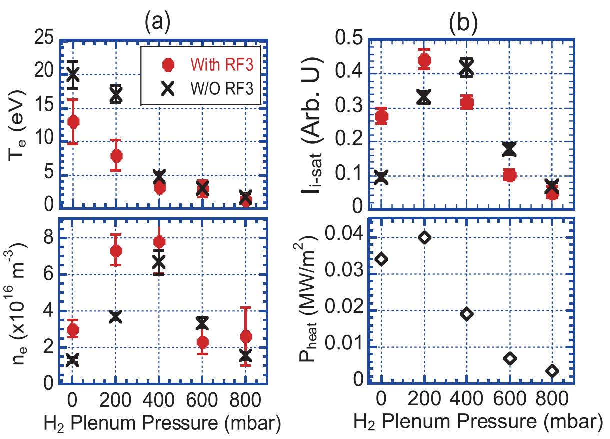

Fig. 4 The dependence of n_e and T_e (a) heat and ion fluxes (b) on the plenum pressure of H_2.

The electron temperature on the target plate reduces to about 1.5 eV by only H_2 injection. These results indicate that the end-loss plasma goes to the plasma detachment state. However, electron ion recombination (EIR) is small at high temperature (T_e > 1 eV). The reason for reduction of the heat flux and ion saturation current on the target plate might be due to the molecular activated recombination (MAR) [13].

3.2 Simultaneous injection of Ar and H_2

In the Ar injection experiments, H_2 gas has been injected simultaneously to examine the effect of molecular process on detached plasma formation. In this case, Ar plenum pressure is fixed at 500 mbar, while H_2 plenum pressure is changed from 0 to 800 mbar. The distribution of heat flux on Z axis is plotted in Fig. 5. Under the simultaneous injection of Ar and H_2, the reduction of heat flux is observed at all point. At Z = 1086 cm, the heat flux reduces from about 0.094 MW/m^2 to 0.005 MW/m^{2}as the plenum pressure increases from 0 to 800 mbar. On the other hand, heat flux at the corner of V-shaped target (Z = 1091 cm) reduces from 0.034 MW/m^2 to 0.0025 MW/m^2. In the case of without gas injection, the heat flux at the corner of the target was found to 0.034 MW/m^2.

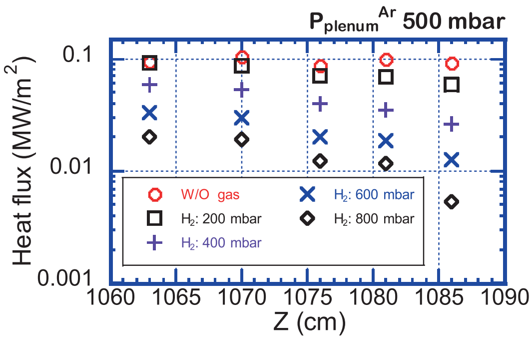

Fig. 5 Heat flux distribution on Z axis.

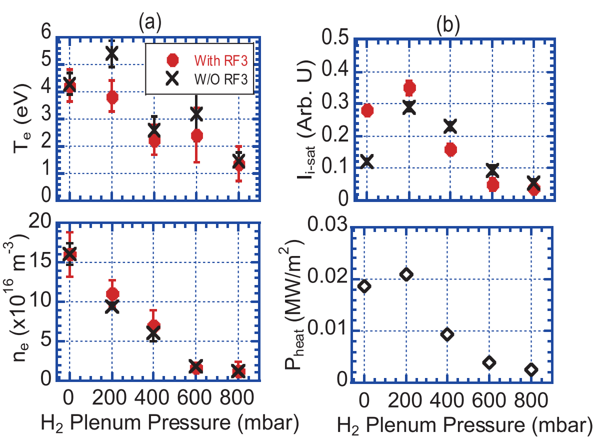

Fig. 6 The dependence of n_e and T_e (a) heat and ion fluxes (b) on the plenum pressure of H_2 under the condition of Ar injection of 500 mbar.

In Fig. 6, measured ion flux, heat flux, electron density, electron temperature are plotted as a function of H_2 plenum pressure. The dependence of heat and ion fluxes at the corner of the target is shown as a function of plenum pressure in Fig. 6 (b). The increase of ion flux firstly occurs due to the H_2 injection. Then decrease of ion flux is observed according to the increase of injecting H_2 gas. According to the increase of H_2 gas injection, the heat flux also decreases. Reduction of heat and ion fluxes in case of only H_2 injection is lower than that of simultaneous injection of Ar and H_2, which indicates the radiation cooling effect of Ar. Ion flux shows a roll over phenomenon. For Ar, it is seemed that ionization is the dominant process because electron density at the corner of the target rises from about 3.0×10^{16} m^{-3} (during RF3) to 1.6×10^{17} m^{-3}.

From the ion flux and electron density, it is estimated that the flow velocity is reduced about 6 times due to Ar injection. According to the increase of H_2 injection, electron density reduces to about 1.2×10^{16} m^{-3}, which indicates that the recombination is also enhanced due to the Ar injection. The electron temperature on the target plate reduces to about 1.3 eV during simultaneous injection of Ar and H_2 injection as shown in Fig. 6 (a). In the GAMMA10/PDX plasma, ion temperature is considerably high. Therefore, the heat received by calorimeter is dominated by ion due to high ion temperature. Ion energy at corner E_i is calculated by the following procedure.

$$E_i = \frac{\textit{Heat flux at the corner}}{\textit{Ion flux at the corner}}. \quad (1)$$

In this calculation, the effect of electron temperature is ignored because of low electron temperature compare to ion temperature (typical value is about 100 eV). The calculated result of ion energy is shown in Fig. 7. At lower H_2 injection (≤ 400 mbar), ion energy reduces almost linearly. However, in the case of higher gas throughput (> 400 mbar), ion energy becomes saturated. It is important to investigate the physical mechanism of the reduction of ion energy due to gas injection. For H_2 injection only, charge-exchange is thought to be a dominant process. On the other hand, in the case of simultaneous injection of Ar and H_2, it is assumed that processes of ion energy loss by the ion-electron collision, charge-exchange and radiation cooling effect of Ar impurity gas. More detailed investigation is needed to clarify the above processes.

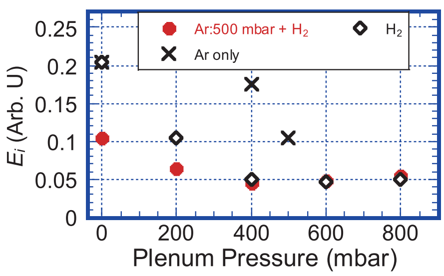

Fig. 7 Ion energy as a function of plenum pressure.

4. Summary

Investigation of heat and ion fluxes have been performed by injecting gas into the D-module of GAMMA 10/PDX. We measured heat flux in the cases of only H_2 injection, only Ar injection and simultaneous injection of both H_2 and Ar experiments. Electron temperature, ion energy, heat and ion fluxes on the target plate decrease with increasing amount of gas injection. These results indicate radiation cooling and formation of detached plasma due to gas injection. Simultaneous injection of noble gas and hydrogen gas showed the most effective results on detached plasma generation. In the future work, we will try to investigate the detachment experiment under the high heat flux circumstance. We will try to make up data base based on the experimental results of GAMMA10/PDX towards the extrapolatable data for ITER (or DEMO). In addition, we have a plan to perform numerical simulation by using standard B2 code [14] in order to understand the various physical mechanism of detachment.

Acknowledgements

This study was supported by the bidirectional collaboration research program of the University of Tsukuba, Osaka Prefecture University, National Institute for Fusion Science (NIFS12KUGM066, NIFS14KUGM086). The authors would like to thank the members of the GAMMA 10 group.

[1] J. Roth *et al.*, J. Nucl. Mater. **390-391**, 1 (2009).
[2] R.A. Pitts *et al.*, J. Nucl. Mater. **415**, S957 (2011).
[3] M. Inutake *et al.*, Phys. Rev. Lett. **55**, 939 (1985).
[4] T. Tamano *et al.*, Phys. Plasmas **2**, 2321 (1995).
[5] Y. Nakashima *et al.*, J. Nucl. Mater. **438**, S738 (2013).
[6] Y. Nakashima *et al.*, Trans. Fusion Sci. Technol. **63**, 100 (2013).
[7] Y. Nakashima *et al.*, Trans. Fusion Sci. Technol. **68**, 28 (2015).
[8] M. Iwamoto *et al.*, Plasma Fusion Res. **9**, 3402121 (2014).
[9] Y. Nakashima *et al.*, Fusion Eng. Des. **85**, 956 (2010).
[10] Y. Ugajin *et al.*, Trans. Fusion Sci. Technol. **63**, 268 (2013).
[11] T. Yokoyama *et al.*, Plasma Fusion Res. **7**, 2402136 (2012).
[12] Y. Saito *et al.*, Trans. Fusion Sci. Technol. **63**, 277 (2013).
[13] A. Pigarov *et al.*, Phys. Lett. A **222**, 251 (1996).
[14] B.J. Braams, NET Rep. **68** EUR-FU/XII-80/87/68 (1987).